J. Phys. D: Appl. Phys. **42** (2009) 075411 (8pp) doi:10.1088/0022-3727/42/7/075411

Microwave and infrared dielectric properties of $Sr_{1-3x/2}Ce_xTiO_3$ (x = 0.154–0.400) incipient ferroelectrics at cryogenic temperatures

Roberto L Moreira[1], Ricardo P S M Lobo[2], Ganesanpotti Subodh[3], Mailadil T Sebastian[3], Mohan V Jacob[4] and Anderson Dias[5]

[1] Departamento de Física, ICEx, Universidade Federal de Minas Gerais, CP 702, Belo Horizonte MG, 30123-970, Brazil
[2] Laboratoire Photons et Matière (CNRS – UPR5), ESPCI, Université Pierre et Marie Curie, 10 rue Vauquelin, 75231 Cedex 05, Paris France
[3] Materials and Minerals Division, NIIST, Trivandrum-695 019, India
[4] Electronic Material Research Lab, School of Engineering, James Cook University, Townsville, QLD, 4811, Australia
[5] Departamento de Química, Universidade Federal de Ouro Preto, Campus Morro do Cruzeiro, ICEB II, Ouro Preto-MG, 35400-000, Brazil

E-mail: bmoreira@fisica.ufmg.br

Received 1 December 2008, in final form 29 January 2009
Published 13 March 2009
Online at stacks.iop.org/JPhysD/42/075411

Abstract

$Sr_{1-3x/2}Ce_xTiO_3$ (x = 0.154–0.400) or $Sr_{2+n}Ce_2Ti_{5+n}O_{15+3n}$ ($n \leqslant 8$) ceramics were prepared by the mixed oxide route. The microwave (MW) dielectric properties of the compounds were investigated in the temperature range from 8 to 295 K. The permittivity increases for decreasing temperatures and saturates below 30 K, following Barrett's equation, demonstrating the incipient ferroelectric nature of the investigated materials. The dielectric loss tangent decreases for decreasing temperatures, reaching a minimum at about 80–120 K, and again increases with further cooling due to the rotations of TiO_6 octahedra. Infrared-reflectivity data show that the dielectric response of the system is driven by the lowest-frequency polar (soft) mode, particularly at lower temperatures, where the phonons become practically uncoupled. The results help us to understand why $Sr_{1-3x/2}Ce_xTiO_3$ materials present more appropriate dielectric properties for MW tunable applications, compared with pure $SrTiO_3$.

(Some figures in this article are in colour only in the electronic version)

1. Introduction

Displacive ferroelectrics contain a group of incipient ferroelectrics or low-temperature ferroelectrics having a variety of interesting properties and microwave (MW) tunable applications [1, 2]. The relative permittivity of incipient ferroelectrics increases for decreasing temperatures and, after reaching a maximum value, it saturates, indicating the absence of a ferroelectric transition. The best known incipient ferroelectrics with a perovskite structure are $SrTiO_3$, $CaTiO_3$ and $KTaO_3$ [1]. Considerable interest has been devoted to the investigation of the dielectric properties of $SrTiO_3$ [2–4], $CaTiO_3$ [5, 6] and $KTaO_3$ [7, 8] and their solid solutions at cryogenic temperatures due to their potential towards practical MW tunable applications. It is well known that the anomalous dielectric behaviour of $SrTiO_3$ can deliver useful applications in microelectronics. The recent developments in high temperature superconductivity increased the demand for MW cryoelectronics [9]. Hence, the search for novel materials with improved properties at low temperatures is still going on.

Recently, Subodh *et al* [10] reported the crystal structure and MW dielectric properties of $Sr_{1-3x/2}Ce_xTiO_3$

($x = 0.133$–0.400) ceramics, or $Sr_{2+n}Ce_2Ti_{5+n}O_{15+3n}$ (SCT), at room temperature. XPS studies revealed that more than 90% of Ce is in the trivalent state [10]. Structural investigations using x-ray diffraction (XRD) [10] and vibrational spectroscopy [11] indicated a pseudocubic symmetry for the SCT ceramics. However, neutron and electron diffraction analyses on SCT by Ubic *et al* [12] revealed a local symmetry lowering to $R\bar{3}c$ due to octahedral tilting ($a^-a^-a^-$, according to Glazer's notation [13]). These materials present relatively high room-temperature permittivities (between 113 and 185), low dielectric losses ($<10^{-4}$) and low temperature coefficients of the resonance frequency ($\tau_f < 700\,\mathrm{ppm\,^\circ C^{-1}}$). The incipient ferroelectric nature and low-temperature applications of $SrTiO_3$ led us to investigate the cryogenic dielectric properties of these materials, as the latter ones are indeed A-site substituted $SrTiO_3$. In this work, we report on the MW and infrared dielectric response of the SCT ceramics at cryogenic temperatures. The results show that these materials constitute an interesting alternative to pure strontium titanate for useful MW tunable applications in low temperature circuitry and devices, owing to their relatively more stable dielectric permittivities, lower dielectric losses and lower τ_f.

2. Experimental

The materials were prepared by the conventional solid-state ceramic route. The ball-milled, dried powder mixtures were calcined at 1100 °C, for 5 h, and sintered for 2 h at 1375 °C, except for the samples $x = 0.400$ (sintering temperature $T_s = 1300\,^\circ C$) and $x = 0.154$ ($T_s = 1400\,^\circ C$). Sintered samples were thermally etched for 20 min at a temperature of about 25 °C below the sintering temperature, and the microstructure was studied by using a scanning electron microscope (JSM 5600-LV, Tokyo, Japan). The phase purity of the ceramics was confirmed through XRD [10]. Cylindrical samples 9 mm in diameter and 4–5 mm in height were used for MW measurements. A $SrTiO_3$ single crystal (CrysTec GmbH) was also investigated, for comparison. The experimental setup used for the MW dielectric characterization of the samples at cryogenic temperatures consisted of a network analyser (E8364B Agilent Technologies), a closed cycle refrigerator (ARSCryo DE210SF) with a temperature controller (Lakeshore 340) and a two-stage vacuum pump. The MW dielectric properties of the samples were measured around their resonance frequencies, lying in the range 2–4 GHz, at temperatures from 8 to 295 K. It is worth mentioning that the exact measuring frequency depends on the sample's dimension and shape, but for non-polar centro-symmetrical materials such as the present ones the dielectric response is practically frequency independent in the region of practical interest (0.8–8 GHz). The S-parameters (S_{21}, S_{11} and S_{22}) around various resonances were measured employing the simplified transmission mode Q-factor (TMQF) technique [14], which accounts for noise. The delay due to non-calibrated transmission lines and its frequency dependence and cross-talk in measurement data were used for data processing. This procedure provided accurate values of Q_L and the coupling coefficients β_1 and β_2 [14]. The unloaded quality factor (Q_u) was subsequently calculated using the equation

$$Q_u = Q_L(1 + \beta_1 + \beta_2). \quad (1)$$

Fourier-transform infrared-reflectivity (FTIR) spectra in the far infrared region (20–700 $\mathrm{cm^{-1}}$) were obtained with a Bruker IFS66v spectrometer within the following configuration: Hg source, Si beamsplitter, liquid-He-cooled Si bolometer and polypropylene windows. For the mid-infrared region (500–4000 $\mathrm{cm^{-1}}$), a globar source, a KBr : Ge beamsplitter, a liquid-N_2-cooled HgCdTe detector and KSR5 windows were used. In both cases, low-temperature measurements were performed in an ARS He-tran cryostat at quasi-normal incidence (8°). Prior to the measurements, the samples were polished to an optical grade with diamond paste (down to 0.25 μm). In order to improve the quality of the reflectivity spectra, reference data were obtained after *in situ* gold evaporation on the measured sample surface [15]. The experimental resolution was better than 4 $\mathrm{cm^{-1}}$ and the beamwidth was 3 mm. The FTIR spectra were fitted by a four-parameter semi-quantum (FPSQ) model [16].

3. Results and discussion

Figure 1 depicts the microstructures of thermally etched SCT ($x = 0.286$ and $x = 0.154$) ceramics sintered at 1375 °C and 1400 °C, respectively. The microstructures show a uniform distribution of grains, which are about 5–10 μm in size. For all the investigated compositions, the microstructures are nearly the same (homogeneous grains with regular shapes and tonalities, characteristics of single phase), except for slight variations in the grain sizes. Both XRD patterns and microstructures did not show the presence of any secondary phases (see also [10]). The sample with $x = 0.154$ has relatively smaller grains compared with $x = 0.286$, even though the sintering temperature for the first sample ($x = 0.154$, 1400 °C) was slightly higher than for the latest one ($x = 0.286$, 1375 °C). This result holds for all compositions, i.e. the grain sizes are larger for increasing x, leading us to conclude that Ce ions act increasing the ceramic grain size. The stripes seen on the grains appear to be growth striations.

Figure 2 shows the relative MW permittivity of the SCT ceramics as a function of temperature. In the case of a normal dielectric material, as the temperature decreases, the permittivity should decrease due to the lowering of phonon interactions. However, in the case of SCT ceramics (all compositions), the permittivity increases for decreasing temperatures and reaches a maximum at about 30 K and then levels off. Similar behaviour was observed in $SrTiO_3$, $CaTiO_3$, $KTaO_3$ and their solid solutions [2–8]. The nonlinear interaction of the optical phonons is the reason for the high permittivity values of incipient ferroelectrics at cryogenic temperatures. In these materials, as the temperature decreases, the soft phonon mode presents an incomplete softening, levelling off at low temperatures due to zero-temperature vibration of the light oxygen atoms, which prevents the long-range ferroelectric order and the corresponding permittivity

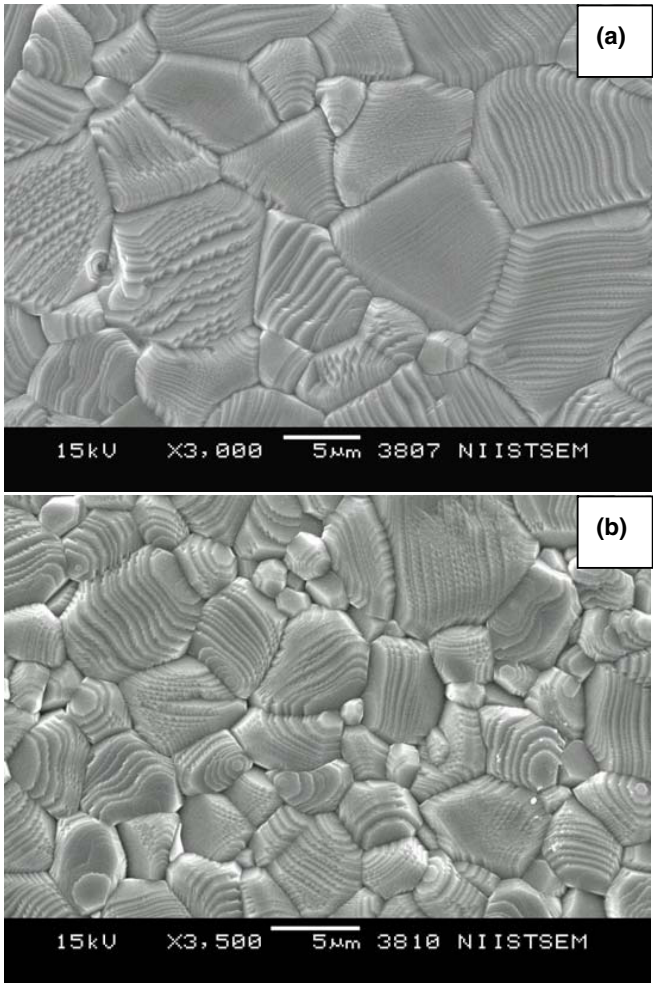

Figure 1. SEM images of $Sr_{1-3x/2}Ce_xTiO_3$ ceramics for (*a*) $x = 0.286$ and (*b*) $x = 0.154$ sintered at 1375 °C and 1400 °C, respectively.

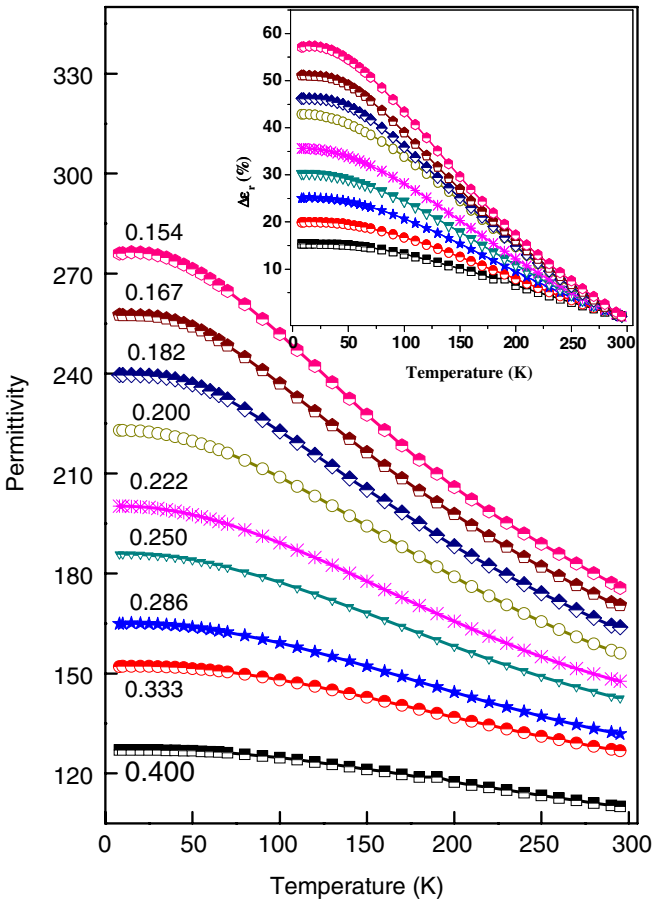

Figure 2. Variation of MW relative permittivities of $Sr_{1-3x/2}Ce_xTiO_3$ ceramics at cryogenic temperatures. Inset: percentage variation in permittivity as a function of temperature.

divergence [3, 17, 18]. Due to this phenomenon, such incipient ferroelectrics are also called quantum paraelectrics. Indeed, the saturation of permittivity and the absence of ferroelectric transition are a consequence of the zero-point energy fluctuations [3, 19].

The inset in figure 2 shows the increase in permittivity (%) from 295 to 8 K for all samples. As a general trend, there is a gradual increase in the permittivity values for decreasing Ce contents. A maximum increase in permittivity is observed for the $x = 0.154$ composition, for which ε_r increases approximately 60% from 295 to 8 K. This is one order of magnitude lower than for $SrTiO_3$ ($x = 0$), where ε_r increases by around 600% (300–20 000) in the same temperature range [3]. Despite the large difference in the absolute values of ε_r for different compositions, the temperature profiles are quite similar. In particular, these curves are very smooth and do not show any anomaly that could indicate phase transitions, although these samples would undergo at least one low-temperature antiferrodistortive transition (AFD) [11], similar to the cubic-tetragonal observed at 110 K in the $SrTiO_3$ single crystal [20, 21]. The absence of such anomaly in SCT compounds is not surprising, since it is also absent in the dielectric response of pure $SrTiO_3$ [3]. This result will be analysed below together with the evolution of the phonon modes around the AFD transition.

Figure 3 shows the variation of the dielectric loss tangent of the SCT materials with temperature. The major sources of dielectric losses in the usual incipient ferroelectrics are [9] (i) fundamental losses connected with multi-phonon scattering of the soft ferroelectric mode; (ii) the transformation of MW electric field oscillation into acoustic oscillation due to electric fields generated by charged defects and (iii) scattering by regions of residual ferroelectricity. In the present case, the dominant factor must be the multi-phonon scattering of the ferroelectric soft mode. The presence of Ce^{4+} ions may act as a charged defect and can also influence the dielectric loss tangent. However, this effect should be very weak, as the materials have a low percentage of Ce^{4+} (4–10% of total Ce, decreasing for smaller x) [10]. It is worth noting that as the temperature decreases the loss tangent decreases, reaching a minimum at temperatures in the range 80–120 K depending on the composition. This behaviour of SCT ceramics can be well correlated with $SrTiO_3$, where a minimum in the dielectric loss is observed at 77 K [4]. The reason for such a minimum in the loss tangent of $SrTiO_3$ is attributed to the rotation of TiO_6 octahedra relative to the Sr ion sublattice. However, the rotation angles change below 65 K and hence the loss tangent increases. In the case of SCT ceramics, the maxima dielectric

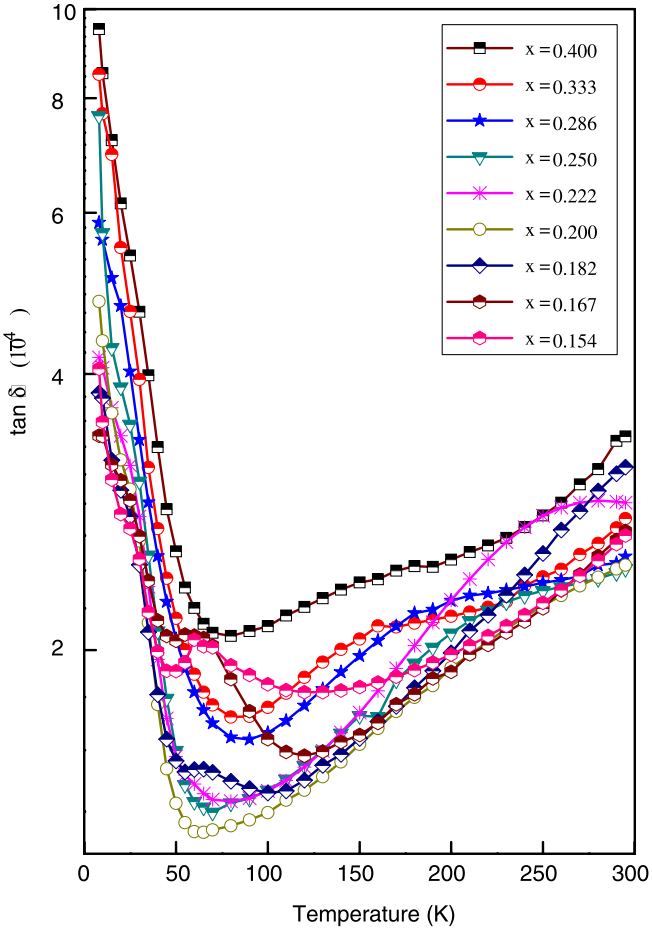

Figure 3. Variation of the MW dielectric loss tangent of $Sr_{1-3x/2}Ce_xTiO_3$ ceramics at cryogenic temperatures.

losses are observed at a lower measured temperatures (8 K), for all compositions. Hence, the low temperature dielectric properties of the SCT ceramics resemble those of $SrTiO_3$ and, therefore, should have the same physical origin as for the pure ($x = 0$) material.

The dielectric properties of incipient ferroelectrics at low temperatures are driven by quantum fluctuations. Barrett [19] derived a simple equation for the permittivity of the incipient ferroelectrics:

$$\varepsilon_r = B + \frac{M}{(T_1/2)\coth(T_1/2T) - T_0}, \qquad (2)$$

where T_1 is the temperature of the crossover between classical and quantum behaviour, T_0 is the Curie–Weiss temperature, M is a Curie–Weiss-like constant and B is a temperature independent parameter. This latest parameter corresponds to the asymptotic ε_r value at a high temperature, and, therefore, it should be close to the Clausius–Mosotti dielectric constant (which does not take into account the dynamics of the ferroelectric soft mode, reflected only in the temperature dependent part of equation (2)). The values of the parameters obtained by fitting the experimental permittivity (figure 2) of the SCT ceramics with Barrett's equation are given in table 1. In order to obtain a higher accuracy of the remaining three parameters (M, T_0 and T_1), we have used fixed B values, equal to the Clausius–Mosotti dielectric constants, calculated in [11]. The negative values of T_0 for SCT samples indicate hypothetical lattice instability at negative temperatures [17, 18]. The Curie–Weiss temperature (T_0) decreases with increasing x. This result indicates that the paralelectric phase becomes more stable with the addition of Ce ions. Similar results were obtained by Lemanov *et al* [5] in Pb-substituted $CaTiO_3$. However, for the present SCT ceramics, a complete ferroelectric transition is absent. It is to be noted that T_1, the temperature of crossover between classical and quantum behaviour, decreases with a decrease in the Ce content. However, the value of T_1 is unusually high compared with that observed for $SrTiO_3$ [3]. The values obtained for B and M are comparable to those of earlier reports [5, 17, 18].

Table 1. Fitting parameters of Barrett's equation for $Sr_{1-3x/2}Ce_xTiO_3$ ceramics.

Sample (x)	B ±0.2	M (10^3 K)	T_1 (K)	T_0 (K)
0.400	34.6	74.3 ± 1.0	274.4 ± 5.7	−667.1 ± 13.3
0.333	37.2	76.9 ± 0.6	245.0 ± 3.5	−547.7 ± 7.1
0.286	37.1	70.4 ± 0.7	236.5 ± 4.0	−433.8 ± 7.1
0.250	37.5	71.5 ± 0.8	221.6 ± 4.5	−373.0 ± 7.2
0.222	37.4	68.9 ± 0.8	212.5 ± 4.8	−319.0 ± 7.0
0.200	37.6	65.2 ± 0.9	225.2 ± 5.3	−241.4 ± 7.0
0.182	38.2	67.8 ± 0.3	206.2 ± 2.0	−234.4 ± 2.6
0.167	38.8	68.8 ± 0.2	195.6 ± 1.3	−217.1 ± 1.6
0.154	39.0	67.8 ± 0.4	193.5 ± 2.4	−189.7 ± 2.8
0 ($SrTiO_3$)[a]	40.0	80	80	35.5

[a] Data from [3, 11, 19].
Note: B parameters fixed according to the Clausius–Mosotti values from [11].

Once the dielectric constant of the isolating centro-symmetrical materials is completely determined by the behaviour of their polar phonon modes, we undertake FTIR measurements of SCT materials. The room-temperature infrared-reflectivity spectra of all samples are presented in figure 4 (circles). The spectra were vertically upshifted (for decreasing x) for the sake of clarity. First, it can be observed that for all samples the spectra are dominated by three main reflections, corresponding to the three phonon modes characteristic of cubic $SrTiO_3$ [22–24]. Indeed, according to Raman and infrared spectroscopic data at room temperature, SCT materials with $x \leqslant 0.400$ would belong to an average cubic symmetry similar to the ideal perovskite structure of $SrTiO_3$ [11]. For this structure, three triply degenerated infrared modes are the only optically active phonons at the Brillouin-zone centre. Because of the large TO–LO splitting, the Lorentz dispersion equation does not hold for this system. Therefore, in order to study the phonon evolutions with composition and temperature, the FPSQ model must be applied [16, 24]. Within the framework of the FPSQ model, the complex dielectric function $\varepsilon(\omega)$ is given by

$$\varepsilon(\omega) = \varepsilon_\infty \prod_{j=1}^{N} \frac{\Omega_{j,\mathrm{LO}}^2 - \omega^2 + \mathrm{i}\omega\gamma_{j,\mathrm{LO}}}{\Omega_{j,\mathrm{TO}}^2 - \omega^2 + \mathrm{i}\omega\gamma_{j,\mathrm{TO}}}, \qquad (3)$$

where ε_∞ is the dielectric constant due to the electronic polarization contribution, $\Omega_{j,\mathrm{LO}}(\Omega_{j,\mathrm{TO}})$ and $\gamma_{j,\mathrm{LO}}(\gamma_{j,\mathrm{TO}})$ are

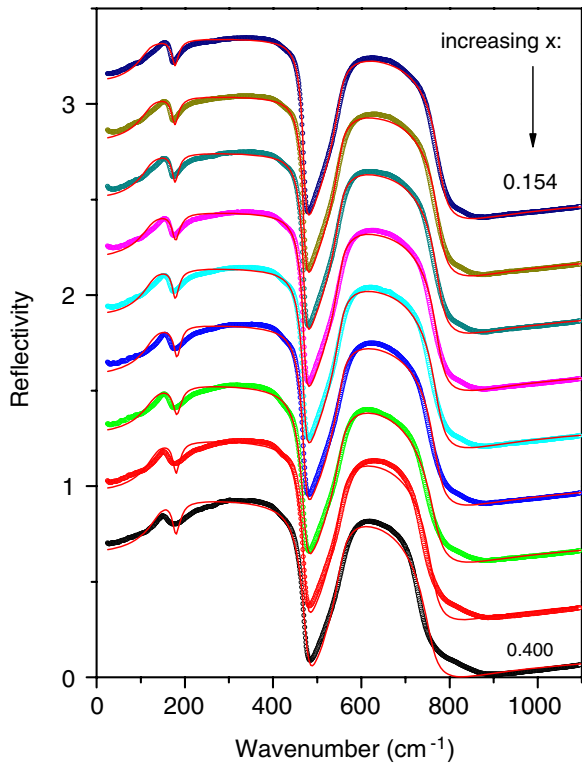

Figure 4. Infrared-reflectivity spectra (circles) with corresponding fitting by the four-parameter semi-quantum model (curves), for $Sr_{1-3x/2}Ce_xTiO_3$ ceramic samples of the two preceding figures. The spectra were vertically upshifted (+0.3) for clarity.

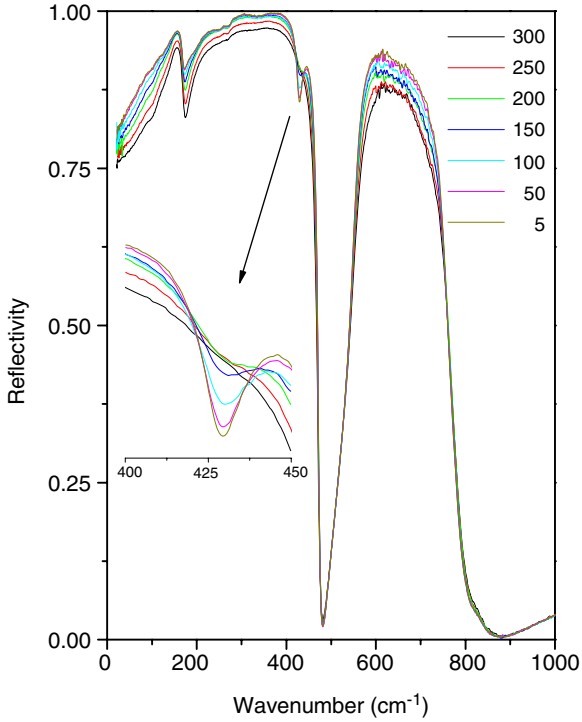

Figure 5. Low-temperature infrared-reflectivity spectra of the ceramic sample with $x = 0.154$ (the temperatures, in K, are indicated). The inset shows a detail around the AFD phase transition.

the frequency and damping of the jth longitudinal (transverse) optical modes, respectively, and N is the number of polar phonons. At quasi-normal incidence, the dielectric function is related to the optical reflectance R by the Fresnel formula:

$$R = \left| \frac{\sqrt{\varepsilon(\omega)} - 1}{\sqrt{\varepsilon(\omega)} + 1} \right|^2. \tag{4}$$

Once the infrared modes are determined, the dielectric strengths of the individual jth TO modes can be obtained by

$$\Delta\varepsilon_j = \frac{\varepsilon_\infty}{\Omega^2_{j,\mathrm{TO}}} \times \frac{\prod_k (\Omega^2_{k,\mathrm{LO}} - \Omega^2_{j,\mathrm{TO}})}{\prod_{k\neq j} (\Omega^2_{k,\mathrm{TO}} - \Omega^2_{j,\mathrm{TO}})}. \tag{5}$$

Now the static (infrared) dielectric constant, which corresponds to the intrinsic MW dielectric constant, can be obtained by adding the dielectric strengths over all modes, i.e.

$$\varepsilon_0 = \varepsilon_\infty + \sum_{j=i}^{N} \Delta\varepsilon_j. \tag{6}$$

The spectra of figure 4 were then adjusted by this model and the fitting curves are presented as solid lines.

The three phonon modes depicted from the spectra of figure 4 account completely for the description of the room-temperature dielectric constant of the SCT system. Indeed, as shown in [11], the hardening of the TO modes, particularly of the lowest-frequency mode, with increasing Ce content, is responsible for the decrease in the overall dielectric permittivity of these materials. Now we are interested in the low-temperature behaviour of the observed polar modes. Figure 5 presents the low-temperature infrared-reflectivity spectra of the ceramic sample with $x = 0.154$, taken as example for several temperatures. By decreasing the temperatures, the main observed features by visual inspection are: (i) an overall increase in the reflectivity, mainly due to the decrease in phonon damping; (ii) the levelling of the reflectivity value at lower wavenumbers, probably linked to the softening of the lowest-frequency mode; and (iii) the appearance of a dip at around 430 cm^{-1}. This dip is characteristic of the cubic ($Pm\bar{3}m$) to tetragonal ($I4/mcm$) AFD transition that occurs around 110 K in pure $SrTiO_3$ [20, 21]. The inset in figure 5 shows a detailed view of the dip region. Notice that for this sample the signature of the AFD transition appears between 200 and 250 K.

Low-temperature FTIR spectra were also obtained for the ceramics with $x = 0.200$, 0.286 and 0.400. These samples presented the same overall behaviour as the $x = 0.154$ of figure 5. In order to investigate the evolution of their phonon characteristics, we have fitted the low-temperature spectra with the FPSQ model, by using only three main phonon modes, which account for the main overall spectra evolution. By using this procedure, we are neglecting any contribution of the dip at around 430 cm^{-1} for the dielectric response of the system. This can be done because this dip constitutes a faint anomaly in the reflectivity with a small dielectric strength [25, 26]. Another comment concerning the AFD of the SCT ceramics is as follows: in all cases, this transition seems to be rather diffuse, maybe occurring in a large temperature interval, which

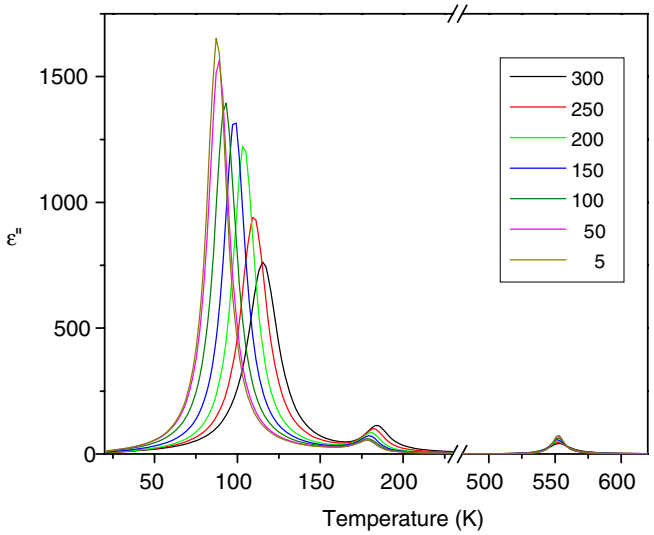

Figure 6. Imaginary part of the infrared dielectric response of the $x = 0.154$ sample, obtained from the fits of the low-temperature FTIR data.

increases with x (just above 200 K, for $x = 0.154$, to room temperature, for $x = 0.400$).

From the fits of the FTIR data for different compositions and temperatures, we could investigate the dielectric response of the system. It is worth noting that for decreasing temperature, as well as for decreasing x, all modes become narrower, indicating decreasing anharmonicity with both parameters. However, the most important result concerns the behaviour of the lowest-frequency soft mode. Once the imaginary part of the dielectric permittivity gives the positions of the TO modes, we show in figure 6 the ε'' spectra obtained from the fits of the low-temperature FTIR, for the $x = 0.154$ sample. This figure clearly shows the softening of the lowest frequency mode (TO1), but also some softening is discerned for the other higher frequency modes, indicating some coupling between the unstable TO1 and the 'hard' TO2 and TO4 modes (the phonon nomenclature is the historical one for strontium titanate) [21, 23].

In order to quantify the coupling between the phonon modes and the soft-mode contribution ($\Delta\varepsilon_1$) to the 'static' dielectric permittivity (ε_0), we present in figure 7(a) the temperature evolution of these parameters, for several samples. These values were obtained with the fitting parameters by using the equations (5) and (6), respectively. We note first the close resemblance between the curve profiles and the absolute values of ε_0 (infrared, figure 7(a)) and ε_r (MW, figure 2) data, indicating that the MW dielectric response of the system is completely driven by the phonon modes. Indeed, the dielectric strength of the phonon TO1 accounts for the larger part of the dielectric response, i.e. this is the mode that controls the dielectric response of the SCT materials. But, as we have pointed out before, the other polar modes also soften at low temperature. Therefore, it is important to know the relative importance of the TO1 mode to the static dielectric response. This can be done by plotting the ratio $\Delta\varepsilon_1/\varepsilon_0$, as shown in figure 7($b$). As can be observed, the TO1 mode is responsible for more than 85% of the static permittivity. Also, with

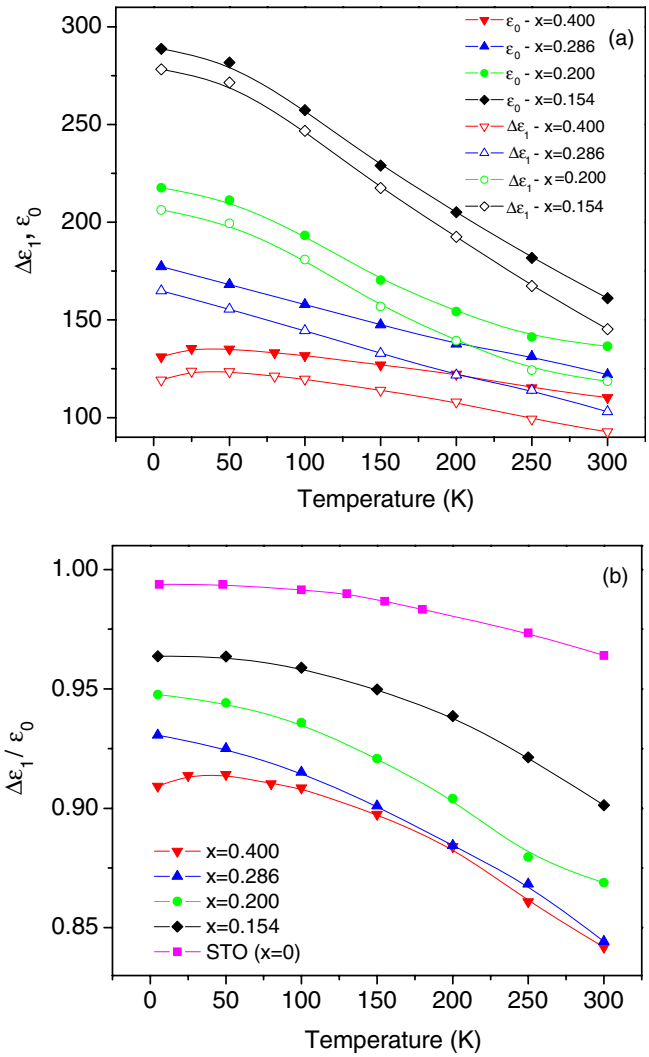

Figure 7. (a) Temperature dependence of the 'static' infrared dielectric permittivity (ε_0) and the dielectric strength of the lowest-frequency mode ($\Delta\varepsilon_1$), for several x values. (b) Relative weight of the soft-mode dielectric strength ($\Delta\varepsilon_1$) to the total 'static' infrared permittivity (ε_0). Data for $SrTiO_3$ are shown for comparison.

increasing x and/or temperature, the TO1-mode contribution to ε_0 decreases.

The temperature dependence of the $\Delta\varepsilon_1/\varepsilon_0$ ratio suggests that the phonon–phonon coupling may be varying. This picture can be further analysed from a standpoint of the f-sum rule [27]. It states that the sum of the oscillator strengths ($\Sigma f_i = \Sigma\Omega_i^2\Delta\varepsilon_i$) is proportional to the total ionic charge and, therefore, should be temperature independent. We have verified that, within the experimental accuracy, the f-sum rule holds for all the samples investigated here. In figure 8(a), we present the results of the individual oscillator strengths (f_i) and their sum (Σf) for the sample $x = 0.154$. We note that, besides Σf, f_4 is also almost temperature independent. On the other hand, the temperature variations and the coupling between phonons 1 and 2 are clear from figure 8(a). In fact, increasing the temperature also increases the coupling of these phonons, in the sense that the charge transfer between them is enhanced. In order to quantify this transference and to summarize the data

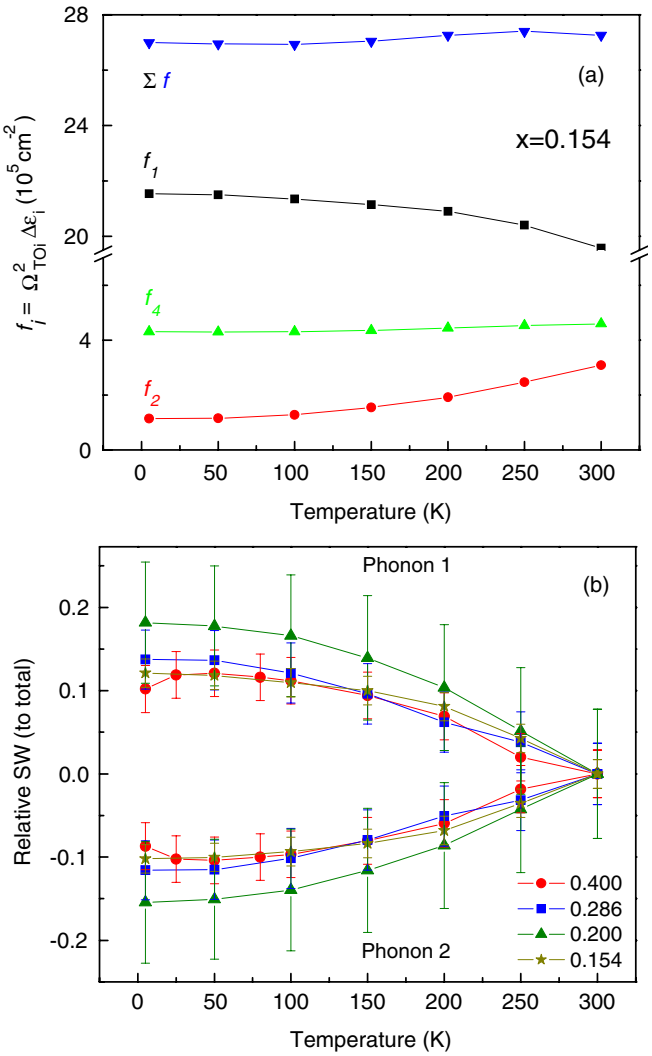

Figure 8. (*a*) Temperature variation of the individual and total oscillator strengths (f_i) of the three main polar modes of the ceramic with $x = 0.154$. (*b*) Temperature evolution of the relative spectral weights ($f_i/\Sigma f$) for the two lowest-frequency polar modes of $Sr_{1-3x/2}Ce_xTiO_3$ ceramics, for the indicated compositions. The estimated error bars are shown.

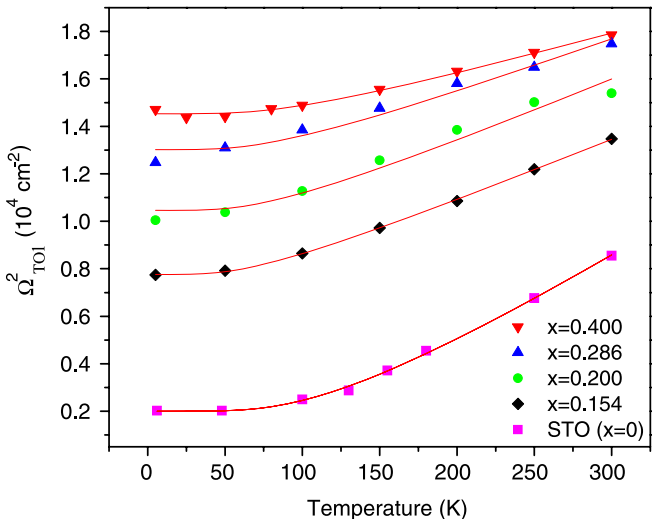

Figure 9. Temperature dependence of the square of the lowest-frequency transverse mode for chosen $Sr_{1-3x/2}Ce_xTiO_3$ ceramics and $SrTiO_3$ single crystal (symbols), fitted by a Barrett-derived expression (lines).

Table 2. Fitting parameters of Mikaki's equation for $Sr_{1-3x/2}Ce_xTiO_3$ ceramics (T_1 values are from table 1).

Material (x)	A (cm^{-2})	T_1 (K)	T_0 (K)
0.400	18.5 ± 0.6	274.4 ± 5.7	-648 ± 27
0.286	23.7 ± 1.8	236.5 ± 4.0	-431 ± 49
0.200	27.4 ± 2.3	225.2 ± 5.3	-268 ± 39
0.154	26.6 ± 0.2	193.5 ± 2.4	-195.1 ± 2.8

for different samples, we present in figure 8(*b*) the relative spectral weights ($f/\Sigma f$) of phonons 1 and 2, normalized to their values at 300 K. The charge and oscillator strength transfer due to the coupling between phonons 1 and 2 is clearly seen for all samples. Figure 8(*b*) also shows that, within the experimental accuracy, the transfer is of the same order for all samples (around 10–15%). These results are not incompatible with those shown in figure 7(*b*), where we have seen that the fractional contribution of the dielectric strengths of phonon 1 ($\Delta\varepsilon_1/\ \varepsilon_0$) is different and smaller for higher x. Indeed, since Ω^2_{TO1} increases with x, this compensates the fractional contribution of the oscillator strengths ($\Omega_i^2\Delta\varepsilon_i$) to the total strength (Σf).

The results of figure 8 (below 100 K, the phonons are uncoupled within the validity of the f-sum rule) besides those from figure 7 ($\Delta\varepsilon_1$ controls the dielectric response of the system) lead us to discuss the temperature behaviour of the soft mode position. Indeed, assuming that the temperature dependence of the static permittivity is caused only by the variations of the TO1 mode and using the Lyddane–Sachs–Teller relationship [16] together with Barrett's equation (equation (2)), we can easily obtain

$$\Omega^2_{TO1} = A[(T_1/2)\coth(T_1/2T) - T_0] \qquad (7)$$

for the soft-mode temperature variation for an incipient ferroelectric (Minaki's equation) [17, 18, 28]. The TO1 values obtained from our fits of the SCT samples together with the adjusted curves to equation (7) are shown in figure 9 and the fitting parameters in table 2. In these procedures, we preferred to use fixed T_1 values (those obtained from the dielectric fits, see table 1) to increase the accuracy in the extrapolated T_0 values. The values obtained for the virtual Curie–Weiss temperatures (T_0) from the dielectric (table 1) and optical (table 2) data present a very good agreement, confirming that the incipient ferroelectric behaviour of the SCT system is caused by the softening of its lower-frequency polar phonon mode.

4. Conclusions

The low-temperature dielectric properties of $Sr_{1-3x/2}Ce_xTiO_3$ ($x \leqslant 0.400$) were measured at MW (2–4 GHz) and infrared (20–4000 cm^{-1} or 0.6–120 THz) regions. It has been shown by both techniques that the static dielectric permittivity of all samples presents typical behaviour of incipient ferroelectric

materials, increasing up to a high saturated value, on cooling. The contribution of the individual polar phonons to the dielectric response was determined and it follows that below 100 K the phonons are relatively uncoupled (whilst coupled above this temperature), while the lowest-frequency phonon mode accounted almost completely for the observed behaviour of the dielectric permittivity. Quantum-mechanical derived expressions for adjusting the MW and infrared data gave close parameters to the soft-mode ferroelectric instability temperature (T_0) and for the crossover temperature between classical and quantum behaviour (T_1). This allowed us to conclude that the SCT system behaves like incipient ferroelectrics with a lower virtual transition temperature (T_0) and a higher crossover temperature (T_1) than classical quantum paraelectrics such as $SrTiO_3$.

Acknowledgments

R L Moreira acknowledges the ESPCI for an invited 'Chaire Joliot' appointment. R P S M Lobo thanks FAPEMIG for an invited position at UFMG. R L Moreira and A Dias are fellows of CNPq and FAPEMIG. G Subodh thanks the Council for Scientific and Industrial Research for the award of Senior Research Fellowship. The authors also acknowledge the facilities offered at JCU under the ARC DP and LIEF schemes to carry out MW characterization.

References

[1] Tagantsev A K, Sherman V O, Astafiev K F, Venkatesh J and Setter N 2003 *J. Electroceram.* **11** 5
[2] Vendik O G and Zubko S P 1997 *J. Appl. Phys.* **82** 4475
[3] Müller K A and Burkard H 1979 *Phys. Rev.* B **19** 3593
[4] Geyer R G, Riddle B, Krupka J and Boatner L A 2005 *J. Appl. Phys.* **97** 104111
[5] Lemanov V V, Sotnikov A V, Smirnova E P, Weihnacht M and Kunze R 1999 *Solid State Commun.* **110** 611
[6] Lemanov V V, Sotnikov A V, Smirnova E P and Weihnacht M 2002 *Appl. Phys. Lett.* **81** 886
[7] Rytz D, Höchli U T and Bilz H 1980 *Phys. Rev.* B **22** 359
[8] Höchli U T and Boatner L A 1979 *Phys. Rev.* B **20** 266
[9] Vendik O G, Ter-Martirosyan L T and Zubko S P 1998 *J. Appl. Phys.* **84** 993
[10] Subodh G, James J, Sebastian M T, Paniago R, Dias A and Moreira R L 2007 *Chem. Mater.* **19** 4077
[11] Moreira R L, Lobo R P S M, Subodh G, Sebastian M T, Matinaga F M and Dias A 2007 *Chem. Mater.* **19** 6548
[12] Ubic R, Subodh G, Sebastian M T, Gout D and Proffen T 2008 *Chem. Mater.* **20** 3127
[13] Glazer A M 1975 *Acta Crystallogr.* A **31** 756
[14] Jacob M V, Mazierska J, Leong K and Krupka J 2001 *IEEE Trans. Microw. Theory Tech.* **49** 2401
[15] Homes C C, Reedyk M, Cradles D A and Timusk T 1993 *Appl. Opt.* **32** 2976
[16] Gervais F and Echegut P 1986 *Incommensurate Phases in Dielectrics - 1. Fundamentals* ed R Blinc and A P Levanyuk (Amsterdam: North-Holland) pp 337–64, chapter 8
[17] Kamba S, Nuzhnyy D, Denisov S, Veljko S, Bovtun M, Savinov M, Petzelt J, Kalnberga M and Sternberg A 2007 *Phys. Rev.* B **76** 054125
[18] Kamba S, Nuzhnyy D, Vanek P, Savinov M, Knizek K, Shen Z, Santava E, Maca K, Sadowski M and Petzelt J 2007 *Eur. Phys. Lett.* **80** 27002
[19] Barrett J H 1952 *Phys. Rev.* **86** 118
[20] Unoki H and Sakudo T 1967 *J. Phys. Soc. Japan* **23** 546
[21] Fleury P A, Scott J F and Worlock J M 1968 *Phys. Rev. Lett.* **21** 16
[22] Barker A S Jr and Tinkham M 1962 *Phys. Rev.* **125** 1527
[23] Spitzer W G, Miller R C, Howarth L E and Kleinman D A 1962 *Phys. Rev.* **126** 1710
[24] Servoin J L, Luspin Y and Gervais F 1980 *Phys. Rev.* **22** 5501
[25] Galzerani J C and Katiyar R S 1982 *Solid State Commun.* **41** 515
[26] Petzelt J, Ostapchuk T, Gregora I, Savinov M, Chvostova D, Liu J and Shen Z 2006 *J. Eur. Ceram. Soc.* **26** 2855
[27] Wooten F 1972 *Optical Properties of Solids* (New York: Academic)
[28] Minaki Y, Kobayashi M, Tsujimi Y, Yagi T, Nakanishi N, Wang R and Itoh M 2003 *J. Korean Phys. Soc.* **42** S1290